Title
THE KINETICS OP VAPORIZATION OP ZINC SINGLE CRYSTALS

Authors
Mar, Raymond W.
Searcy, Alan W.

Publication Date
1970

UCRL-18257 Rev.

c.2

THE KINETICS OF VAPORIZATION OF ZINC SINGLE CRYSTALS

Raymond W. Mar and Alan W. Searcy

January 1970

AEC Contract No. W-7405-eng-48

LAWRENCE RADIATION LABORATORY
UNIVERSITY of CALIFORNIA BERKELEY

25

UCRL-18257 Rev.

DISCLAIMER

THE KINETICS OF VAPORIZATION OF ZINC SINGLE CRYSTALS

Raymond W. Mar* and Alan W. Searcy

Inorganic Materials Research Division, Lawrence Radiation Laboratory, and Department of Materials Science and Engineering, College of Engineering, University of California, Berkeley, California

ABSTRACT

January 1970

The rate of vaporization from (0001) and $(10\bar{1}0)$ surfaces of zinc single crystals have been measured by the torsion-Langmuir method and have been compared to rates of vaporization of zinc from torsion effusion cells. A small concentration of impurities lowers the vaporization coefficient α_v for the (0001) surface to 0.7, but α_v for the $(10\bar{1}0)$ surface of the same material and for the (0001) surface of high purity crystals are unity. The concentration of dislocations that were active in causing thermal etching of the (0001) surfaces was of the order of $10^4/cm^2$ for the samples tested. These experimental results are not in accord with the prediction of the Hirth and Pound model for metal vaporization that $\alpha_v = 1/3$ for low index, low defect surfaces.

At the time this work was done the writers were, respectively, graduate research assistant and professor of materials science.

* Mar is now located with Sandia Laboratories, Sandia Corp., Livermore, California.

INTRODUCTION

Experimental evidence is strong that vaporization of solids proceeds by successive removal of atoms or molecules from ledges that advance across the crystal surfaces from sources such as crystal edges or dislocation sites.[1,2] From the foundation provided by earlier models to describe the stepwise vaporization process, Hirth and Pound have deduced a model that yields quantitative predictions of vaporization rates for metal and non-polar molecular crystals.[3,4,5]

The Hirth and Pound model assumes that the only sources for vapor atoms are self-adsorbed atoms which have diffused onto the surface from monatomic ledges. Crystal edges and screw dislocations act as ready sources of ledges when a crystal is vaporized, and an equilibrium concentration of self-adsorbed atoms is maintained at the ledges. According to the model, the ledges accelerate as they move away from a source across low-index crystal surfaces and a concentration gradient of self-adsorbed atoms is established between successive ledges. The ledge spacing approaches a limiting value, however, at relatively small distances from the source because ledge acceleration approaches zero when ledge spacing is large. Hirth and Pound calculated that the average concentration of self-adsorbed atoms for this steady state ledge spacing is about 1/3 the equilibrium concentration. An important consequence of their model is the prediction that vaporization into vacuum from surfaces of dense atom or non-polar molecule packing (i.e. from most low crystallographic index surfaces), which have low dislocation densities will occur at 1/3 the rate calculated from the Hertz-Knudsen-Langmuir equation,[6] that is

$$J_{obs} = 1/3\ P_{eq}(2\pi mkT)^{-1/2}$$

where J_{obs} is the flux of molecules from the surface, P_{eq} is the equilibrium vapor pressure, m is the molecular weight of the vapor molecules, k is the Boltzmann constant, and T is the absolute temperature. Expressed in customary terminology for vaporization kinetics, the model predicts that the vaporization coefficient, $\alpha_v = J_{obs}/J_{max}$, is 1/3 for perfect close-packed surfaces. In contrast, the model predicts that high index planes, which can be viewed as made up of closely spaced ledges, as well as low index planes with dislocation densities in excess of about 10^6 per cm^2 should have vaporization coefficients of unity.

The derivation of the model is persuasive and its predictions seem generally to be in good agreement with experimental fact. Consequently, the model has been widely accepted, and has been invoked to explain measured rates of vaporization for a number of solids.

When Hirth and Pound first described the model,[5] they noted that Harteck[7] and Eucken[8] had concluded that the vaporization coefficients for silver and copper lie between 1/4 and 1/2. However, Hirth and Pound considered that neither these results nor discordant experiments which indicated α_v to be unity for several metals were conclusive tests of the theory because in none of the experimental studies were surface and experimental conditions sufficiently well defined. Subsequently, Rothberg, Eisenstadt, and Kusch[9] suggested that their experimental value for CsI monomers, $\alpha_v = 0.36\ (+0.14, -0.11)$ agrees with the Hirth and

Pound model. Burns[10] has commented that the limiting expression given by Hirth and Pound seems to apply at the melting points of solid aluminum oxide, gallium oxide, and indium oxide.

Hirth and Pound's own conclusions as of 1963[2] was that vaporization data for a number of systems were consistent with their model, but that alternate interpretations were also possible. In particular, they suggested that the possibility that impurity adsorption reduces measured values of α_v cannot be ruled out in most of the studies. They questioned on this point their own attempt[11] to test with silver the prediction that $\alpha_v = 1/3$ for low dislocation count, low index surfaces on the grounds that the study was made in a relatively poor vacuum (background pressure about 10^{-5} torr). They had found $\alpha_v = 0.4$ for (100) and (111) silver surfaces. Subsequently Winterbottom and Hirth[12] found $\alpha_v = 1$ for silver measured under similar circumstances, but with an improved vacuum. The count of dislocations which were active in producing thermal etch pits for both studies was about $10^6/cm^2$, a level that is high enough according to the Hirth and Pound model so that an evaporation coefficient near unity rather than near 1/3 can be expected.

A satisfactory test of the Hirth and Pound prediction that α_v should be 1/3 for low index planes requires not only that a low dislocation density be demonstrated for the test material, but proof that the results are not confused by impurity effects and convincing evidence that systematic errors in flux and temperature measurements are low. Convincing evidence is difficult to obtain because even equilibrium effusion measurements made by experienced investigators often disagree

by a factor of two or more.[13] For example, from comparison of free surface evaporation rates measured in one laboratory[14] with equilibrium measurements carried out in another,[15] a vaporization coefficient of 0.5 could be derived for BaF_2, but free surface measurements made in the apparatus used for the equilibrium determinations led to $\alpha_v = 0.9 \pm 0.1$.

Experience in our laboratory with several different substances has shown that our apparatus[16] for measurement of equilibrium and free surface vaporization fluxes by the torsion effusion[17] and torsion-Langmuir methods under nearly identical experimental conditions is well suited for determinations of vaporization coefficients. We decided to use the apparatus for an attempt to test the Hirth and Pound model for the basal (0001) planes of zinc. The vapor pressure of zinc is well known[18] and high enough for convenient measurement over a range of temperatures below the melting point. Large zinc crystals of high purity can be grown. Basal surfaces that are relatively free of macroscopic faults can be obtained because of easy basal cleavage of zinc at liquid nitrogen temperatures. The etch pit method can be used to determine dislocation positions and concentrations on the various planes.[19,20] Previous etch pit studies of zinc had shown that dislocation densities lower than 10^5 per cm^2 can be obtained.[20,21]

Formation of zinc oxide on the zinc surface by reaction with residual oxygen or water at the background pressures of about 10^{-7} torr in our systems might reduce the free surface vaporization rate below that characteristic of an uncontaminated surface. We could expect, therefore, to establish only a lower limit to the vaporization coefficient. We doubted the prediction of a temperature independent, low vaporization

coefficient for metals despite the fact that we could point to no flaw in the elegant development of the Hirth and Pound model, and we believed that the risk of obtaining an inconclusive result was worth running.

EXPERIMENTAL

The apparatus used in making torsion-effusion and torsion-Langmuir measurements and techniques of pressure measurement have been described in a previous paper.[16] To improve and lengthen the constant temperature zone for studies at 500° to 700°K, a 7.5 cm diameter cylinder fabricated of 6 mil copper was placed between the torsion cell and the tungsten hairpin heating elements. This arrangement provided a 5 cm zone in which the temperature was constant within 2°.

The temperature of a torsion cell placed in the middle of the constant temperature zone was plotted against the temperature of a chromel-alumel probe thermocouple placed just below the cell to obtain a calibration curve. Temperatures of the cell during vaporization runs were obtained by calculating the true temperature from the calibration curve. The calibration curve was checked periodically throughout the investigation, and no significant change in the curve was ever noticed. The thermocouples were calibrated by measurements of the melting points of lead and tin.

Equilibrium data and free surface sublimation data were both collected with essentially the same graphite cell. For torsion-Langmuir studies, single crystal zinc wafers were placed behind drilled graphite plates at the positions of the orifices in effusion studies. Corrections were made for the effect of the short tubular channels on the measured pressures.[22] Holes in the top of the cell used for torsion-Langmuir

measurements reduced the possibility that zinc which evaporated from the rear faces of the crystal wafers might escape in a manner that would contribute significantly to the measured torque.

The apparatus was used as a null point device. To ensure that no extraneous leaks contributed to the measured torque, assemblies which contained zinc samples but in which no orifices were drilled were heated to temperatures of 620°K. No significant deflections were found.

Rod shaped crystals 1 cm in diameter were grown under argon in graphite molds by the Bridgeman technique with the plane of interest perpendicular to the growth axis. The major impurities detected spectrographically in these crystals were 8×10^{-4} % copper and 5×10^{-5} % silver.

A single crystal purchased from Semi-Elements Inc. was also used. Their crystal was a 1.3 cm diameter rod grown by the Bridgeman technique in a pyrex mold with the rod axis perpendicular to the basal plane. Because rods grown in pyrex molds are susceptible to surface pitting, the rod was acid machined to a 1 cm diameter. All impurities in this sample were below the spectroscopic limit for detection. The commercially purchased zinc will be referred to as high purity zinc since the most obvious difference between the two materials is that the commercial crystal had no spectroscopically detectable impurities.

For preparation of (0001) surfaces, crystal rods were annealed in vacuum at a temperature of 620°K for one hour and then were cleaved at liquid nitrogen temperatures. To reduce contamination from water condensation on the surface, cleaved crystals were transferred to a methyl alcohol bath in a glove box that had been flushed with and bathed in

argon. Crystals were warmed to room temperature in methyl alcohol, were dried in a stream of air, and were stored in a dessicator until used.

Zinc chips from the single crystal specimens were used for the effusion runs. Effusion data were accepted only after at least 10% of the zinc in the cell had evaporated. Torsion-Langmuir measurements reported in this paper are all steady state values. An extensive investigation of the approach to steady state conditions will be reported in a separate paper.

Prismatic $(10\bar{1}0)$ surfaces were prepared from a crystal grown with the prismatic plane oriented perpendicular to the rod axis. Then wafers about 5 mm thick were cut with a spark cutter. The surfaces were mechanically polished with papers of Nos. 0, 00, 000, and 0000. The final polish was performed with a polishing solution of 1μ alumina suspended in kerosene. Polished samples were rinsed in acetone, and stored in a dessicator until used.

The distributions and densities of dislocations intersecting the basal planes were determined by chemical etching with a solution of 0.5M HBr in ethanol.[19] The usual etching procedure was to dip the crystal into the etchant for about 5 seconds with the surface of interest facing upward. The etched crystal was washed in ethanol and dried in a stream of air.

EFFUSION AND TORSION-LANGMUIR RESULTS

The effusion results plotted in Fig. 1 showed no significant dependence on sample source, orifice geometry, or torsion wire diameter. A least squares fit of the data yields

$$\log P_{atm} = - (6.683 \pm .095) \frac{10^3}{T} + 5.893 \pm (.029) \qquad (1)$$

This equation is represented by the dotted line of Fig. 1. The average third law heat of sublimation for zinc is calculated to be $\Delta H^\circ_{298} = 31.294 \pm .075$ as compared to $\Delta H^\circ_{298} = 31.245 \pm .050$, reported by Hultgren, Orr, Anderson, and Kelly[18] from a critical evaluation of 15 different experimental studies. The difference in the third law heat of sublimation is only 0.2%, but the small difference, if uncorrected, would produce an 8% error in the value calculated for the vaporization coefficient.

Free surface vaporization measurements are summarized in Table I and Fig. 2. The solid line represents the equilibrium data collected in this investigation. Table I also contains values of α calculated from the ratio of each free surface pressure to the equilibrium pressure given by Eq. (1). The vaporization coefficient measured for the (0001) surface of the high purity zinc averages 1.11 ± .08. These values were collected in a number of runs using four different (0001) surfaces. For the $(10\bar{1}0)$ surface of the lower purity zinc $\alpha = 1.02 \pm .09$. For the (0001) surface of the lower purity zinc $\alpha = .73 \pm .08$. All uncertainties listed are standard deviations from the mean.

The maximum possible value of α_v under steady state conditions for a crystal that has negligible stored energy is 1. The value of 1.11 measured for the (0001) face of the high purity zinc therefore indicates that the errors in determination of α must at least slightly exceed the maximum error of 10% that we would estimate. But convincing evidence that α_v for the (0001) plane of the lower purity zinc was truly less than

unity was obtained by the use of a differential torsion cell. The differential cell had two sets of orifices arranged so that the torque produced by vaporization from a pair of (0001) surfaces of the lower purity zinc opposed the torque produced by vaporization of a pair of $(10\bar{1}0)$ surfaces. Since each orifice was closely similar in dimensions to an orifice of the other pair, any possible errors in absolute pressure measurements which might arise, for example from an unrecognized contribution of surface diffusion, will nearly cancel in these differential measurements. To eliminate the possibility that the direction of orifice orientation or orifice dimensions might cause a significant differential torque, the crystals were interchanged and the measurements were repeated. The orifice dimensions are given in Table II and differential pressure data are summarized in Table III.

If Eq. (1) is accepted as giving the pressure for the $(10\bar{1}0)$ surface, then the (0001) surface for the lower purity zinc is calculated to have an average vaporization coefficient of $0.71 \pm .04$ from these differential runs. This agrees well with $0.73 \pm .08$ calculated from the ratio of torsion-Langmuir to torsion-effucion pressures.

CHEMICAL AND THERMAL ETCH PIT MEASUREMENTS

The experimental vaporization coefficients for the low index crystal faces were clearly higher for all crystals and planes studied than the value 1/3 predicted by the Hirth and Pound theory for perfect, low index crystal surfaces. But the theory predicts that α will be greater than 1/3 for surfaces which are intersected by a high concentration of screw dislocations. High, but different dislocation densities in the lower purity zinc and high purity zinc crystals might explain the high, but

different values of α which were measured for the crystals from the different sources. Since chemical etch pits are believed to form where screw dislocations intercept a surface, chemical etch pit counts were made for six samples of lower purity zinc and three of high purity zinc. Average surface counts ranged from 4×10^4 pits/cm^2 to 2×10^5 pits/cm^2. Some samples displayed high and low etch pit density regions on the same surface, with densities varying from 9×10^3 to 6×10^5 pits/cm^2. Fortunately, the high density regions were usually confined to visibly distorted areas near the edges of the crystal, and the area defined by the orifice could be chosen from the more perfect center portion of the crystal where the pit counts were less than 10^5/cm^2. No consistent differences in the dislocation densities between lower purity and high purity zinc were found.

Thermal pits on cleaved surfaces preferentially formed at cleavage steps, slip lines, and scratches. But pits also formed with random distribution in areas free of visible surface defects. All of the initial pits were roughly hexagonal in cross section, with pits in the high purity zinc more regular than those in the lower purity zinc.

The concentration of thermal pits observed for various lower purity (0001) zinc surfaces initially ranged from 1.0×10^3 to 3.0×10^4 pits/cm^2 and did not increase with time of heating; for high purity zinc the initial concentration ranged from 9×10^3 to 4×10^4 pits/cm^2 and increased to 1 to 3×10^5 as steady state was approached.

MORPHOLOGY OF SURFACES DURING STEADY STATE SUBLIMATION

Surfaces were examined at various magnifications with an optical microscope and with a scanning electron microscope. Here we will describe only the steady state surfaces that developed for the regions of surface exposed by orifices through graphite masking plates. Surface recession was negligible in the masked regions and the luster of the cleaved surface was maintained. The (0001) steady state surfaces of the lower purity and high purity zinc were distinctly different from each other and from the $(10\bar{1}0)$ surface.

The (0001) surfaces of the high purity zinc looked like flat plains traversed by interconnecting ridges. A typical steady state surface is shown in Fig. 3. The features varied slightly from sample to sample. On some, the ridges graded smoothly into the flat areas as on Fig. 3, and on others there was a sharper transition from the base of a ridge to the plain.

In contrast, a typical steady state (0001) surface of the lower purity zinc showed large macroscopic pits in a relatively flat surface.[4a-b] The number and size of these pits varied with time for any given surface even though no corresponding variation in measured pressures could be detected.

Any given pit broadened with time of heating until its rim touched the rims of other pits (Figs. 4a-4e). Flat plateaus then widened from the points at which the pit rims had touched[4f] until the formation and spread of new pits caused a new recession of the plateau regions.

Throughout the period of sublimation many 1 to 3μ diameter hexagonal pits (Fig. 5) were visible on both the flat plateau surfaces and in the

pitted areas of the lower purity zinc. Concentrations of these pits ranged from 3×10^6 pits/cm^2 to 1×10^7 pits/cm^2, but it is apparent that these pits are not active as sources of evaporation ledges because the ledges of the large thermal pits recede at rates that are not perturbed by movement past the small pits. The shapes of the small pits are those that would minimize their surface energies. Similar features could not be seen on the (0001) surfaces of the high purity zinc.

The macroscopic pits that formed during the cyclical process of pit growth and plateau growth during steady state vaporization originated from starting pits which were very steep sided and superficially appeared to emanate from the inactive 1 to 3μ diameter pits just described but that were probably dislocation sites. With time, these steep sided pits developed flat bottomed macroscopic pits like those shown in Fig. 5. A macroscopic pit developed only if the penetration depth was large before the pit started to flatten. About one out of every ten starting pits ever achieved macroscopic proportions.

$(10\bar{1}0)$ surfaces were characterized by arrays of generally parallel ridges or tilted ledges. Smaller rib-like ledges ran in bands perpendicular to the direction of the major striations. (Fig. 7).

Throughout any period of the steady state vaporization, particles that appeared dark in the optical micrographs and light in the electron micrographs could be seen to grow as flaky, loose clusters from the surface. The particles were so loosely held on non-pitted surface regions that a stream of air was sufficient to remove most of them. The particles were usually detached during the preparation for the electron

microscope. Observations with an optical microscope showed the white ridge areas of Fig. 3 to be regions where the particles collected and partially masked sublimation of the high purity zinc. The particles formed in surface patches and along ledges in the walls of pits of the lower purity zinc, and at the tops of the peaks on the $(10\bar{1}0)$ surfaces. Ledge motion in the growth of macroscopic pits is somewhat hindered by these particles (Fig. 8), but many of the particles were remarkably mobile and were pulled along by the prismatic side faces of ordinary pits.

A microprobe analysis of the particles gave no indication that they contained carbon or measurable amounts of metallic elements other than zinc, but this result is not conclusive because the microprobe method is relatively insensitive for carbon analysis and is not well suited to analyzing rough surfaces. This material is not likely to be carbon because samples isolated from possible sources of carbon (grown in quartz molds and samples vaporized in alumina cells with alumina orifices) developed the same surface particles as those grown and vaporized in graphite.

For several reasons we believe that the particles are ZnO, produced by continuous reaction of zinc with residual oxygen in the system. At 575°K the reaction is thermodynamically favored for oxygen partial pressures higher than 10^{-50} atm, while during this investigation the total pressure was on the order of 10^{-7} torr.

Surfaces deliberately heated for very long times accumulated large amounts of the particles. An X-ray diffraction pattern was obtained from one such surface. In addition to the principal lines for the basal

surface of zinc, a few extra lines with spacings expected for ZnO were observed. The relative intensities were not those expected for randomly oriented ZnO, but any ZnO that was formed would probably be strongly oriented. The two strongest diffraction intensities corresponded to the (202) and (101) planes of ZnO.

The rate of particle formation on the surface was less dependent on temperature than was the rate of vaporization of zinc. A surface held at about 470°K for more than twelve hours was heavily laden with the particles although the surface recession due to vaporization was relatively small. A sample evaporated at about 620°K for less than 30 minutes underwent greater surface recession, but showed considerably less particle formation.

The temperature dependence is not consistent with the assumption that the particles are impurities from the zinc. For impurities to collect at the surface at a rate faster than the surface receded would require that the impurities, which are at concentrations well below their solubility limits, must diffuse out and precipitate as a new phase. Such behavior would seem thermodynamically impossible. The temperature dependence of particle formation is reasonable if the particles were ZnO formed by the oxidation of zinc, because, for oxidation at low pressures, the rate may be determined primarily by the rate at which oxygen is supplied to the surface.

Observations that at the low oxygen pressures of this study the oxide remained in discrete and loosely held patches provides a partial explanation of why the vaporization rate is not measurably reduced by

oxide formation. The sizes of particles (black in these optical micrographs) increased with time as the pits spread (4a-4e) but was very small again in 4f. The particles at the pit edges grew with time until the macropit boundaries intersected, annihilating the ledge surfaces to which the particles had clung. The particles then probably dropped off the vertically mounted surfaces.

Crystal edges are ready sources for ledges.[1,2] Accordingly, vaporization experiments were performed on lower purity (0001) surfaces with the entire surfaces including edges exposed in order to see what differences in surface morphology might result. The surfaces remained very flat during sublimation. During the course of many runs on separate samples, pits of the sizes shown in Figs. 4c-4f and 6 never developed. Instead, ledges were seen to generate at the crystal edges. Occasionally an area would develop a few small pits of the type shown on Fig. 4b, but these pits never grew larger. Figure 9 shows how most of a lower purity (0001) crystal surface looked. There were no ledge features or pits on the relatively smooth surface. The zinc oxide particles formed in randomly spaced lumps. The surface was flat enough for subgrain reflections to be detected by the naked eye. The steady state vaporization rate measured for a surface with exposed edges was 1.1 times the equilibrium rate. Uncertainty in this value is high because the exposed surface area was difficult to measure precisely. The surface of samples from a different rod that was subjected to the same procedure showed some pit and ledge structure, but no growth of large pits.

High purity zinc samples were also vaporized with the edges exposed. The surface appearance was no different from that of the orifice defined surfaces.

DISCUSSION

The (0001) surfaces for which vaporization rates were measured in this research were shown by chemical etching techniques to be intercepted by 10^4-10^5 dislocations per cm^2. Of these, about one in ten was active in nucleating thermal etch pits for the lower purity zinc and all were apparently active for the high purity zinc.

The fraction of surface area that is close enough to active dislocation sites to yield ledge spacings that are significantly smaller than the steady state values is given by $A_o = \pi(r_a + 5\lambda_o)^2 C$ where r_a is the radius of the area about a dislocation that is affected by capillarity, λ_o is the spacing between ledges far from a ledge source, and C is the number of active dislocations per cm^2.[5] The Hirth and Pound model predicts that only this fraction A_o of the total surface can have a vaporization flux significantly greater than 1/3 J_{max}. The value of r_a can be estimated from $r_a = \gamma V/.01kT$, where γ is the surface tension in ergs per cm^2 and V is the atomic volume. The surface free energy for zinc can be estimated to be 1000 erg/cm^2 from $n\Delta H_{sub}/4N$ where n is the number of atoms per cm^2, ΔH_{sub} is the enthalpy of sublimation and N is Avogadro's number. Assuming the maximum concentration of dislocations that are active in initiating thermal pits to be $3x10^5$ $lines/cm^2$ and $\lambda_o = 2x10^{-6}$, then the maximum value for A_o is $\pi(10^{-5} + 5x2x10^{-6})^2$ $(3x10^5)$ and A_o is less than 10^{-3}. The results that $\alpha_v = 1$ for high purity zinc and $\alpha_v = 0.7$ for the lower purity zinc are, therefore, discordant with the expectation from the Hirth and Pound model that α_v should be about 1/3 for a low index surface with this low dislocation count. The small degree of surface roughness observed for the high purity zinc is

insufficient to raise the measured vaporization flux by more than a few percent.

Contamination of the surface by oxygen or other residual gases of the vacuum system does not provide a means for explaining the discrepancy between the experiments and the Hirth and Pound model. Surface impurities are expected to reduce the vaporization flux, and the micrographic evidence indicates (Fig. 8) that zinc oxide accumulation did slightly reduce vaporization rates where the oxide particles formed.

The reduction of zinc flux in areas physically masked by zinc oxide particles could have been essentially total if transport of zinc in and on the oxide particles were low. But the relatively small reduction in rates of surface recession in physically masked areas is evidence that at least the surface of the oxide maintains a high zinc activity.

But the count of thermal etch pits for the lower purity zinc remained constant at the level established as soon as heating was commenced, in the range of 10^3 to 3×10^4 pits/cm^2, while the count of thermal pits for the high purity zinc increased during the period when the vaporization approached steady state from values near 10^4 to values in the range 1×10^5 to 3×10^5 pits/cm^2. This difference, as well as the differences in steady state surface morphologies and in measured vaporization coefficients, probably reflects a difference in effects of impurities on vaporization because chemical etch pits counts for a higher purity zinc were of the same magnitude as found for the lower purity zinc. Impurities are known to reduce regularities in ledge form and to cause bunching of monatomic ledges. Straighter ledges in the thermal pits of the high purity zinc during the approach to steady state vaporization and the

absence of observable ledges during steady state sublimation support the conclusion that that material had the higher purity.

We conclude that the observations of this study, while qualitatively in good agreement with expectation of the atomistic models for metal vaporization do not confirm the quantitative preduction of the Hirth and Pound model. A source of the discrepancy might be an underestimation of the distance over which ledges must travel before achieving their steady state velocities. Such an interpretation would be consistent with the observation that the thermal etch pit count at the time that steady state vaporization was achieved was lower for the lower purity zinc than for the high purity zinc which gave higher vaporization rates. But when the edges of the (0001) plane were unmasked, the surfaces of some of the lower purity zinc samples remained plane under steady state vaporization instead of showing large thermal pits. This result seems inconsistent with the view that a spacing of ledge sources significantly smaller than the dimensions of the crystal face (i.e. of the order of 1 mm) is required to produce a high value of α_v. The expectation from the Hirth and Pound model is that when movement of ledges from the widely separate crystal edges dominates the kinetics, the value of α_v should decrease toward 1/3. A measurement of flux from a surface with exposed edges, however, yielded an apparent increase of α_v from 0.7 to 1.1. And while the value is uncertain, we do not think it could be as much as 50% above the true value. The effect of edge-domination of the kinetics, therefore, was to increase α_v. And while low index planes were developed near the edges, the greater part of the surface remained close to (0001) in orientation.

Professors Hirth and Pound have each suggested that small deviation in orientation from the close packed plane might give rise to additional monatomic ledge sources.[24] Hirth and Winterbottom suggest an additional possibility that a specific impurity might catalyze disc nucleation on the terraces.[24] Ledges from either of these types of sources could have gone undetected in our study. We believe, however, that the high crystal axial ratio for zinc (1.856) favors nearly perfect basal cleavage and that either of these two explanations is unlikely for a second reason: The rate of approach to steady state vaporization correlates well with the rate of spreading of the ledges which we can observe to be initiated at thermal etch pits. Since the spread of ledges from the sources that we can observe determines the time at which steady state is achieved, it seems somewhat artificial to invoke a second set of sources for the ledges which determine the magnitude of the steady state vaporization flux.

A plausible explanation appears to be that a boundary condition applied in developing the model is not appropriate for the steady state measurements in this study or in other studies to which the model has been applied.[11,12] The model neglects the deceleration of ledges that will result when trains of ledges from different sources collide, and modification of the model to take this deceleration into account leads to the prediction that α_v will be unity as long as ledge generation is rapid.[25]

ACKNOWLEDGMENTS

This work was performed under the auspices of the United States Atomic Energy Commission.

The scanning electron microscope was provided under a grant from the National Science Foundation and kindly made available by Professor Thomas E. Everhart. George Georgakopoulos provided help with the microprobe and Mick Nemienac provided help with the electron microscope. Advice from Dr. D. J. Meschi was very helpful to us. We appreciate comments from Professors Pound and Hirth on a preliminary draft of this paper.

REFERENCES

1. O. Knacke and I. N. Stranski, Prog. Met. Phys. 6, 181 (1956).
2. J. P. Hirth and G. M. Pound, Prog. in Mat'ls. Sci. 11, 7 (1963).
3. J. P. Hirth and G. M. Pound, J. Chem. Phys. 26, 1216 (1947).
4. J. P. Hirth and G. M. Pound, J. Phys. Chem. 64, 619 (1960).
5. J. P. Hirth and G. M. Pound, Acta Met. 5, 649 (1957).
6. See K. D. Carlson in "The Characterization of High Temperature Vapors," J. L. Margrave, Ed., John Wiley & Sons, Inc., New York (1967) Chapt. 5, and R. C. Paule, and J. L. Margrave, ibid, Chapt. 6.
7. B. P. Harteck, Z. Physik Chem. 134 1 (1928).
8. A. Eucken, Metallwirtschaft 15, 27, 63 (1936).
9. G. M. Rothberg, M. Eisenstadt, and P. Kusch, J. Chem. Phys. 30, 517 (1959).
10. R. P. Burns, J. Chem. Phys. 44, 3307 (1966).
11. J. P. Hirth and G. M. Pound, Trans. A.I.M.E. 215, 932 (1959).
12. W. L. Winterbottom and J. P. Hirth in Condensation and Vaporization of Solids, E. Rutner, P. Goldfinger, and J. P. Hirth, Eds., Gordon & Breach, New York (1964) p. 347.
13. H. B. Skinner and A. W. Searcy, J. Phys. Chem. 72, 3375 (1968).
14. R. G. Bautista and J. L. Margrave, J. Phys. Chem. 69, 1770 (1965).
15. P. E. Hart and A. W. Searcy, J. Phys. Chem. 71, 2763 (1966).
16. R. W. Mar and A. W. Searcy, J. Phys. Chem. 71, 888 (1967).
17. M. Vollmer, Z. Physik Chem., Bodenstein Festband, 803 (1931).
18. R. Hultgren, R. L. Orr, P. D. Anderson, and K. K. Kelly, Selected Values of Thermodynamic Properties of Metals and Alloys (John Wiley and Sons, Inc., New York, 1963).

19. H. S. Rosenbaum and M. M. Saffen, J. Appl. Phys. 32, 1866 (1961).

20. J. V. Sharp, Stat. Solidi 8, (1965).

21. A. W. Ruff, J. Chem. Phys. 41, 1204 (1964).

22. R. D. Freeman and A. W. Searcy, J. Chem. Phys. 22, 762 (1954).

23. R. D. Freeman and J. G. Edwards in "The Characterization of High Temperature Vapors," J. E. Margrave, Ed. John Wiley & Sons, Inc. New York (1967) Appendix C.

24. Private Communications, 1969.

25. A. W. Searcy, unpublished work, University of California.

Table I. Free surface sublimation results

Surface	Temperature (°K)	Pressure (atm)	Vaporization Coefficient
(0001)	574	1.915×10^{-6}	1.08
High purity zinc	656	7.847×10^{-7}	1.13
	591	3.981×10^{-6}	1.06
	574	1.967×10^{-6}	1.10
	558	9.605×10^{-7}	1.24
	583	2.676×10^{-6}	1.01
	593	4.067×10^{-6}	.99
	595	4.370×10^{-6}	.98
	546	5.528×10^{-7}	1.29
	530	2.422×10^{-7}	1.21
(0001)	604	5.122×10^{-6}	.74
Lower purity zinc	629	1.511×10^{-5}	.79
	630	1.539×10^{-5}	.56
	578	1.896×10^{-6}	.87
	621	1.109×10^{-5}	.80
	557	1.783×10^{-6}	.85
	558	5.666×10^{-7}	.68
	556	5.149×10^{-7}	.66
	564	8.585×10^{-7}	.75
	546	3.173×10^{-7}	.70
	564	8.999×10^{-7}	.78
	537	2.397×10^{-7}	.81
	531	1.870×10^{-7}	.88
	556	4.814×10^{-7}	.64
	539	2.352×10^{-7}	.74
	560	6.350×10^{-7}	.67
	573	1.264×10^{-6}	.76
	576	1.333×10^{-6}	.69

(Continued next page)

Table I Continued

Surface	Temperature (°K)	Pressure (atm)	Vaporization Coefficient
	572	1.282×10^{-6}	.79
	575	1.240×10^{-6}	.65
	573	1.141×10^{-6}	.69
	575	1.274×10^{-6}	.67
	571	1.011×10^{-6}	.67
	575	1.097×10^{-6}	.57
	517	6.690×10^{-8}	.70
	516	7.797×10^{-8}	.85
	535	1.670×10^{-7}	.67
	563	8.577×10^{-7}	.78
	637	2.298×10^{-7}	.76
$(10\bar{1}0)$	570	1.472×10^{-6}	1.02
Lower purity zinc	611	9.997×10^{-6}	1.07
	529	1.952×10^{-7}	1.02
	534	2.293×10^{-7}	.96
	532	2.189×10^{-7}	1.00
	585	2.635×10^{-6}	.90
	589	3.890×10^{-6}	1.23
	543	4.110×10^{-7}	1.06

Table II. Orifice dimensions used in differential cell

Minimum Orifice Diameter (cm)	Channel length (cm)	Channel angle (degrees)	Orifice correction factor[22,23]	fa**	Σfa
.5236*	.1163	0	.8634	.186	.392
.4862*	.317	60	1.108	.206	
.5234	.1234	0	.8565	.185	.392
.4883	.317	60	1.108	.207	

* The first two orifices were opposed to the second two.

** fa = (force correction factor) (minimum orifice area)

Table III. Differential torsion cell results

Temperature (°K)	$(10\bar{1}0)$ Torque-(0001) torque (deg)	Δ Pressure (atm)	(0001) Evaporation coefficient*
572	15.155	$.62 \times 10^{-6}$	.62
569	14.100	$.57 \times 10^{-6}$	.67
570	13.803	$.55 \times 10^{-6}$	.68
589	18.720	$.94 \times 10^{-6}$	.73
610	38.725	$.20 \times 10^{-5}$	.77
589	12.760	$.64 \times 10^{-6}$	.73
557	4.547	$.23 \times 10^{-6}$	.70
582	12.845	$.65 \times 10^{-6}$	.74
554	3.690	$.19 \times 10^{-6}$	.73

* Based on the assumption that $\alpha_{(10\bar{1}0)} = 1$

FIGURE CAPTIONS

Fig. 1. Effusion results for zinc.

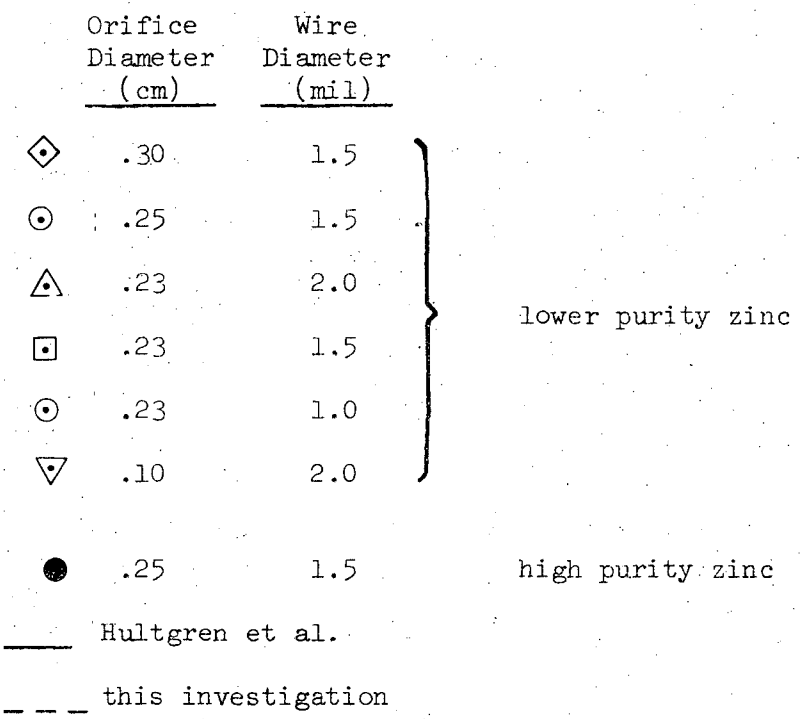

Fig. 2. Free surface sublimation results for zinc.

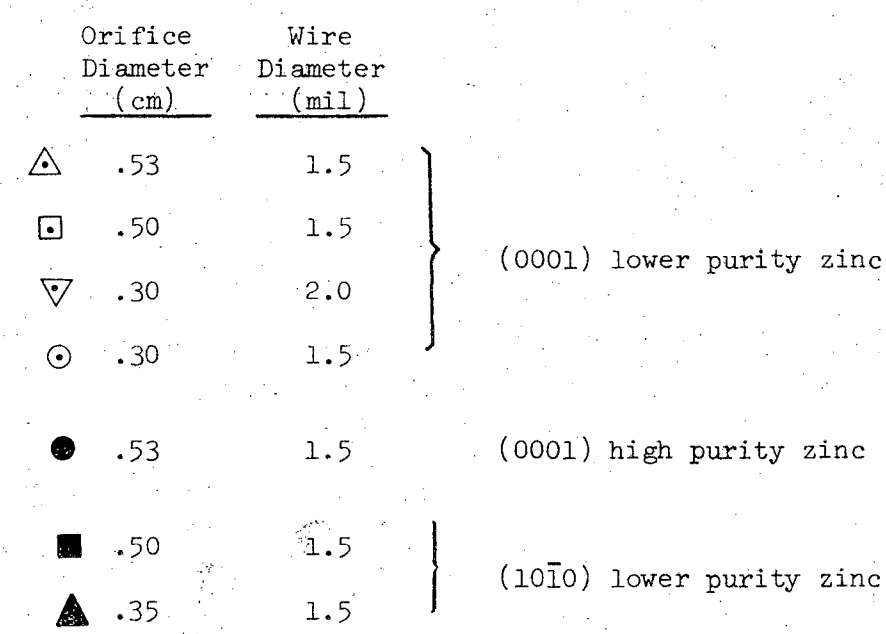

Fig. 3. Steady state (0001) surface high purity zinc.

Fig. 4. Development of (0001) surface of grown zinc during steady state sublimation.

Fig. 5. Flat bottom of one of the macroscopic pits of Fig. 4, showing 1-3 micron diameter inactive pits.

Fig. 6. Pits starting in the (0001) surface of the grown zinc which eventually developed into macroscopic pits.

Fig. 7. Surface development on the $(10\bar{1}0)$ surface of the grown zinc.

Fig. 8. Interaction between evaporation ledges and a second phase particle on the (0001) surface of lower purity zinc.

Fig. 9. (0001) surface of lower purity zinc which sublimed with crystal edges exposed. White patches are believed to be zinc oxide.

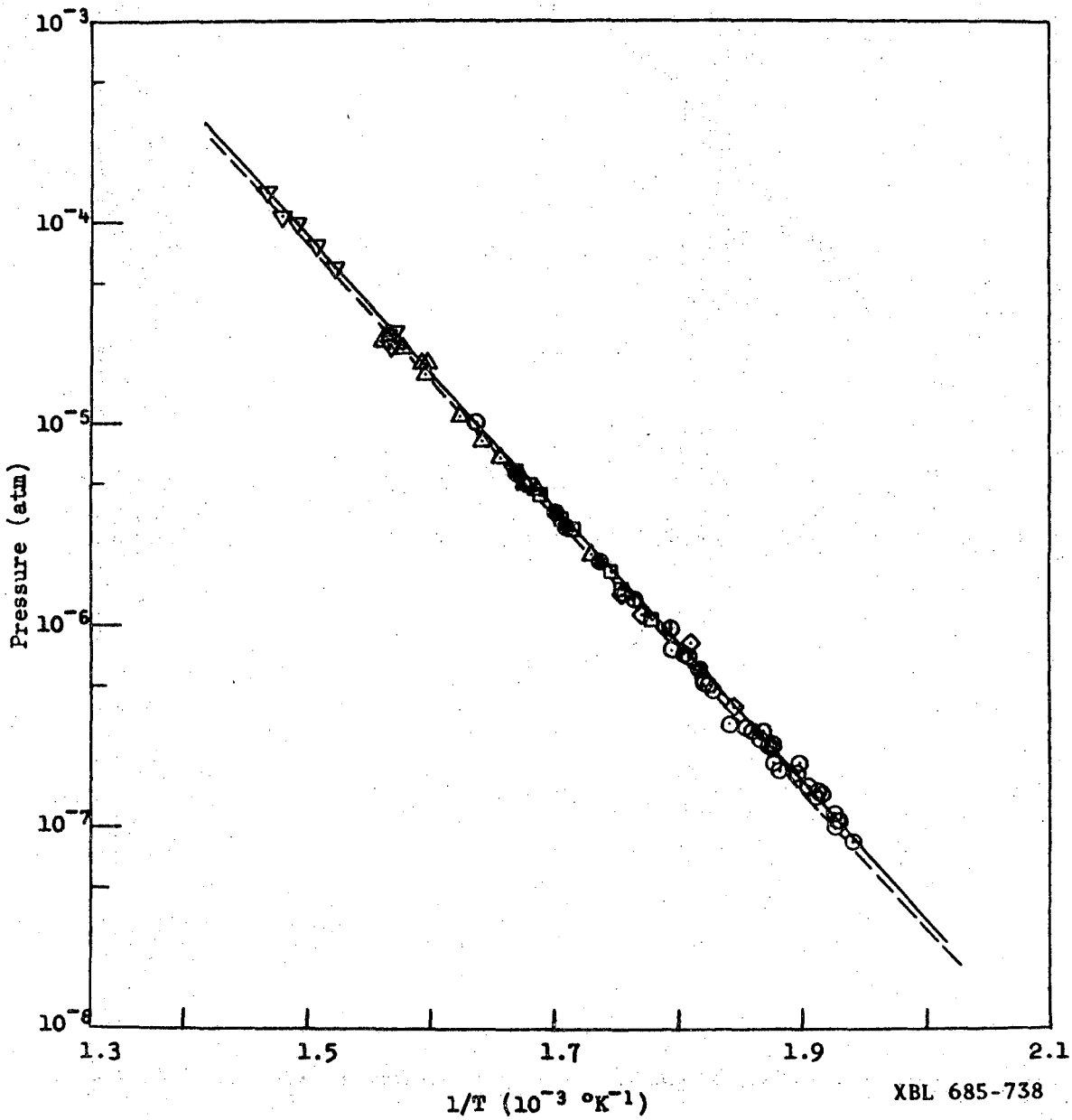
10^{-3}
10^{-4}
10^{-5}
10^{-6}
10^{-7}
10^{-8}
Pressure (atm)
1.3
1.5
1.7
1.9
2.1
1/T (10^{-3} °K^{-1})
XBL 685-738

Fig. 1

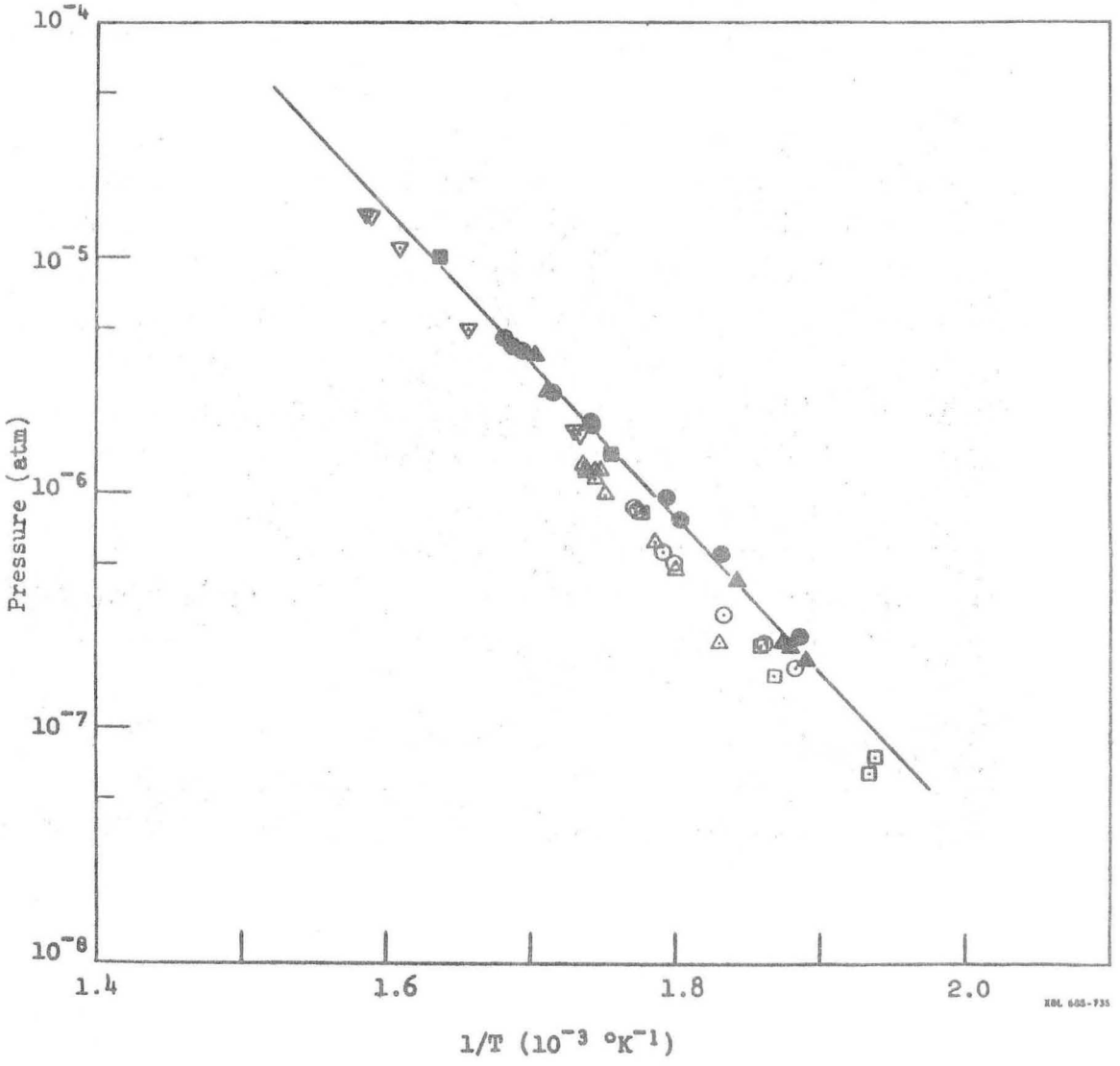

Fig. 2

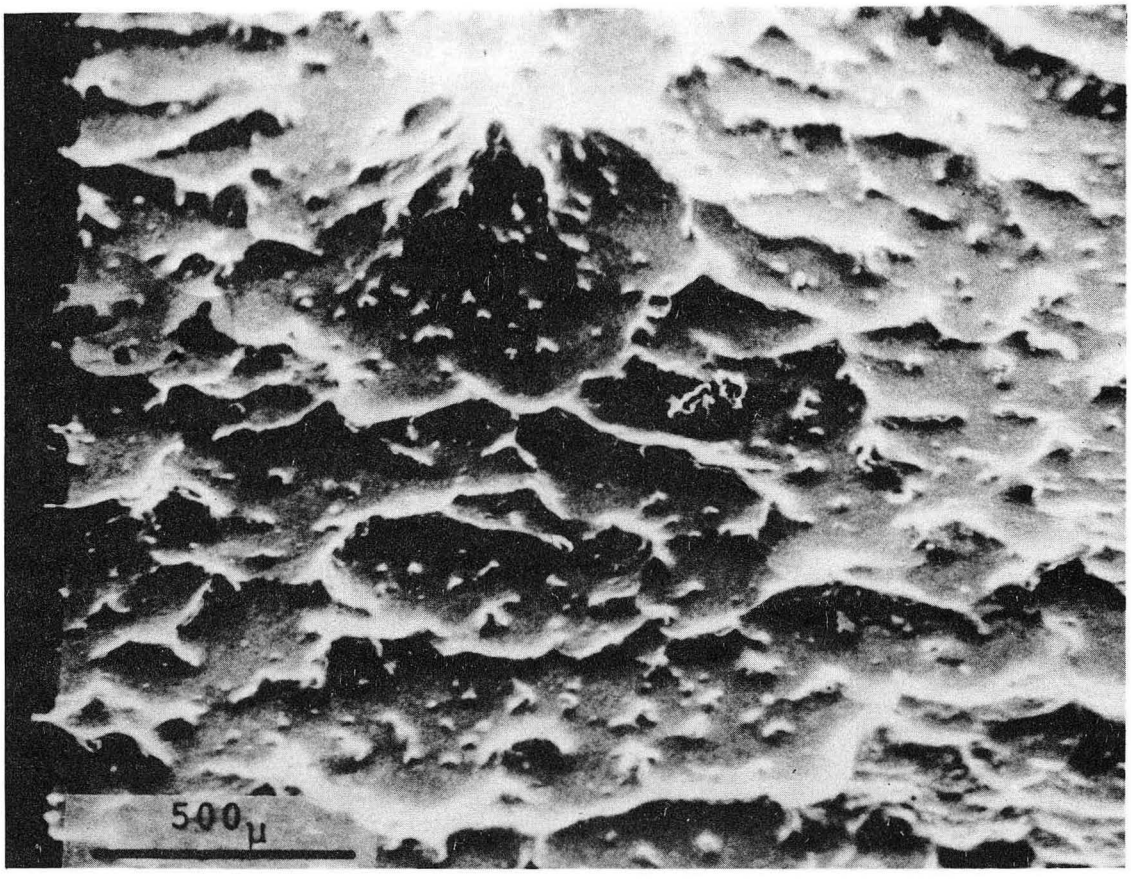

XBB 687-4160

Fig. 3

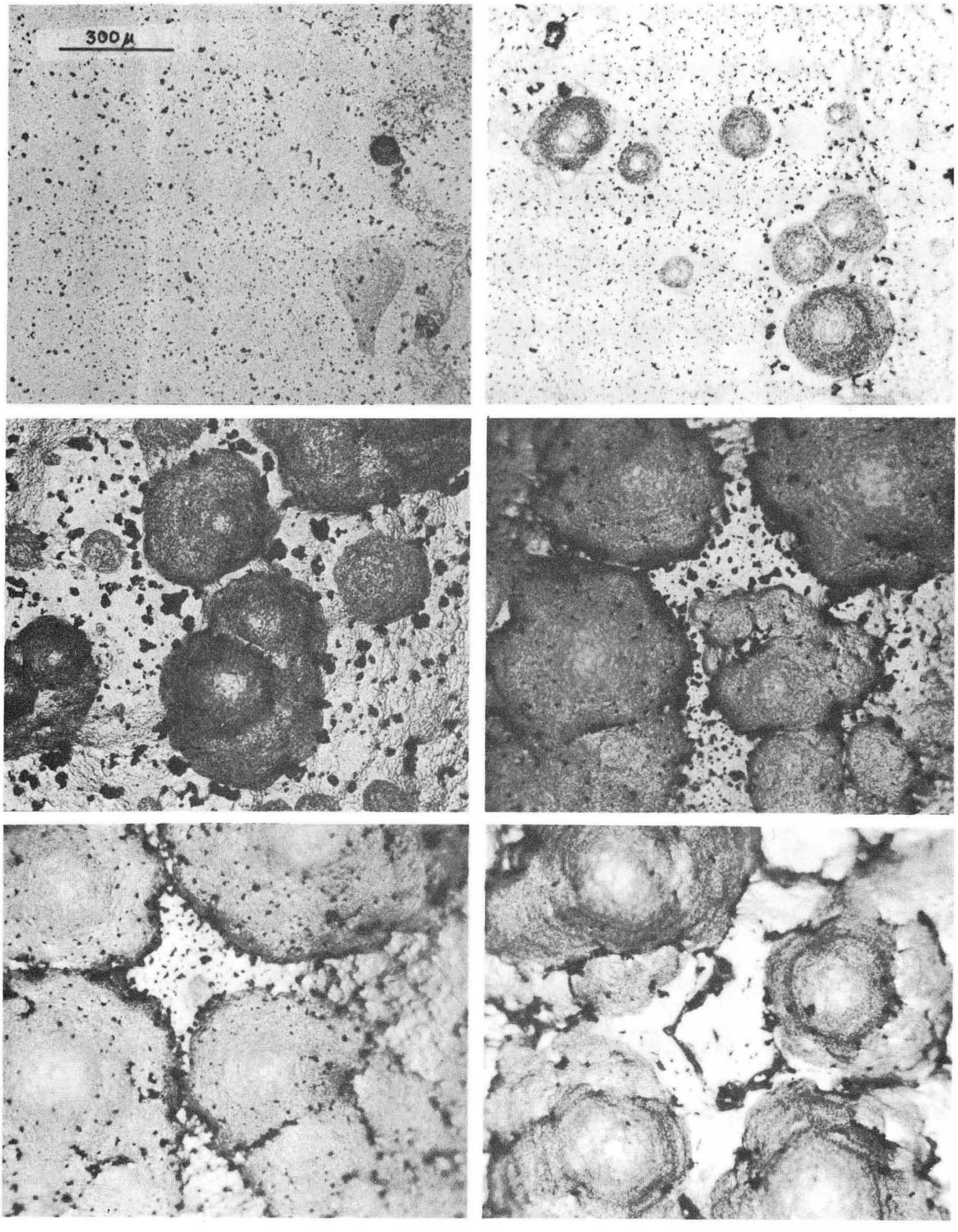

XBB 685-2681

Fig. 4

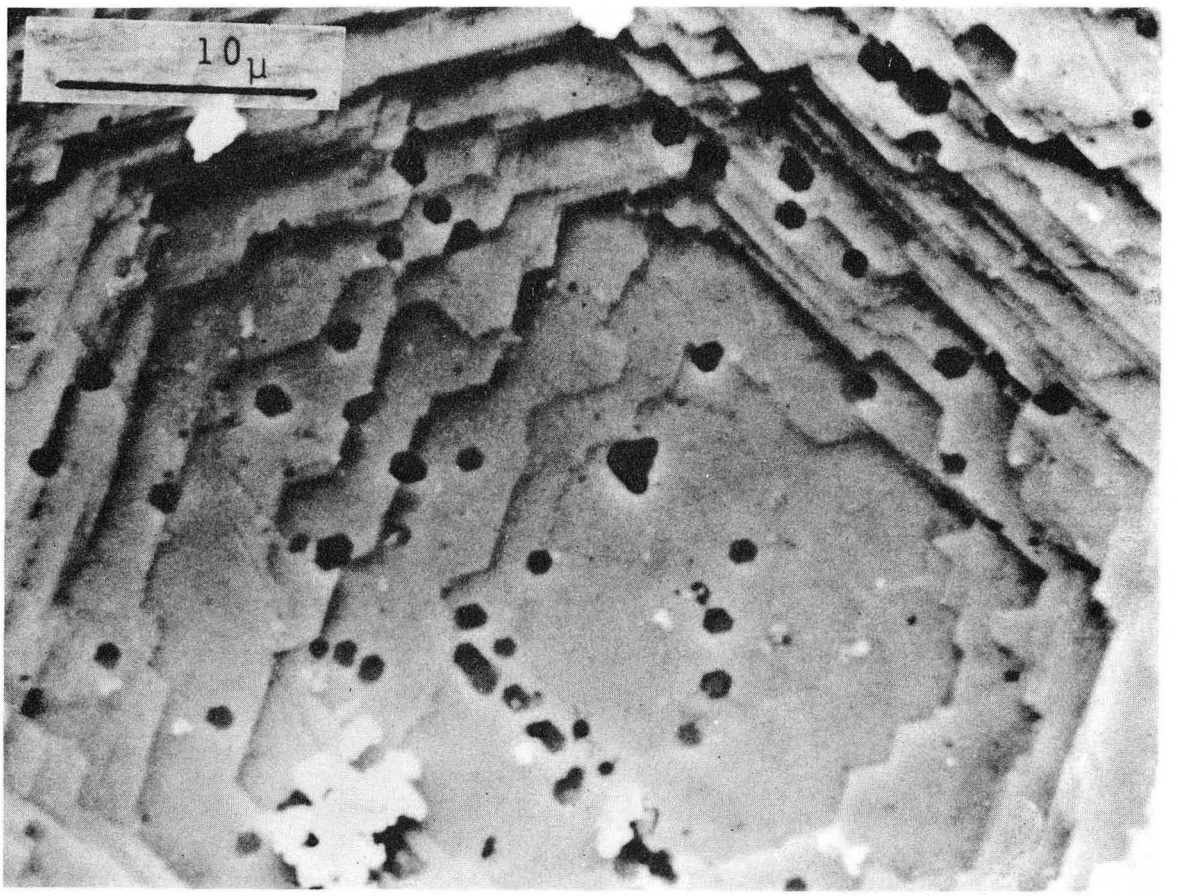

XBB 687-4163

Fig. 5

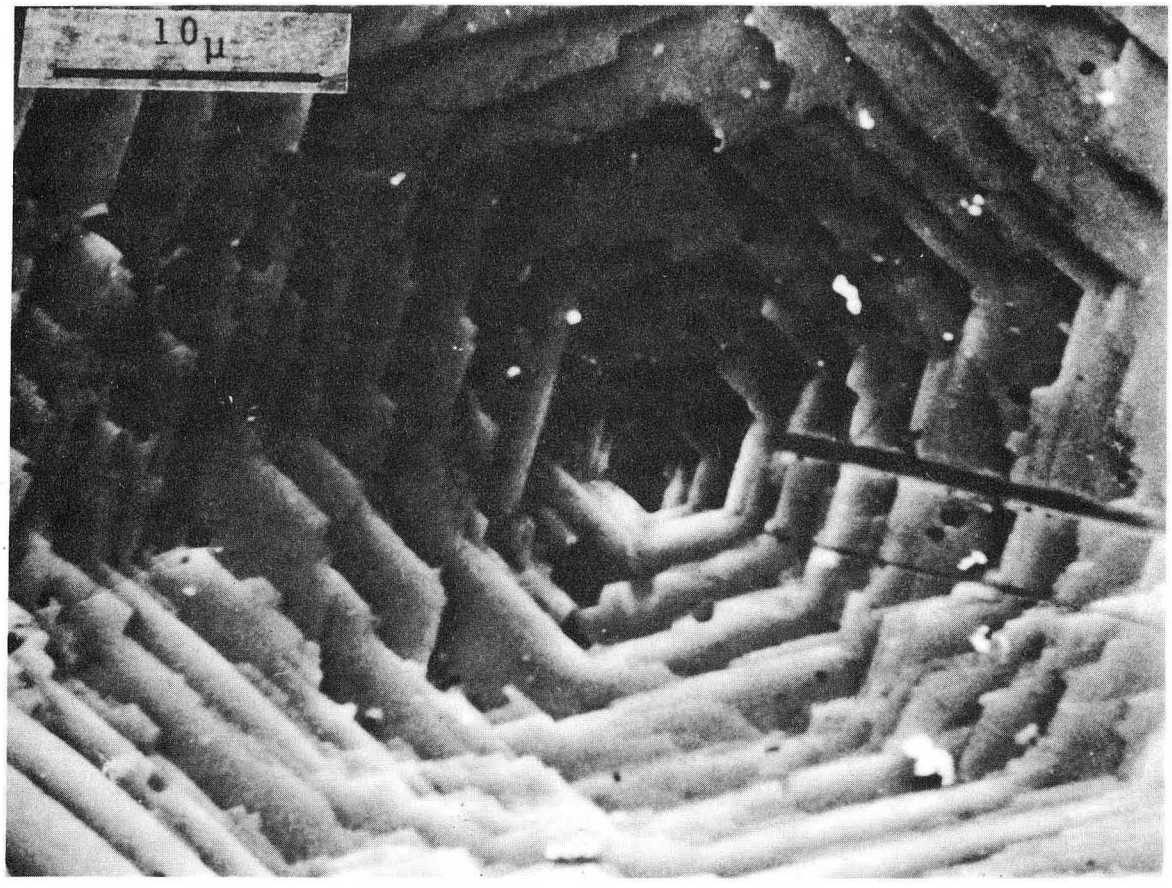

XBB 687-4166

Fig. 6

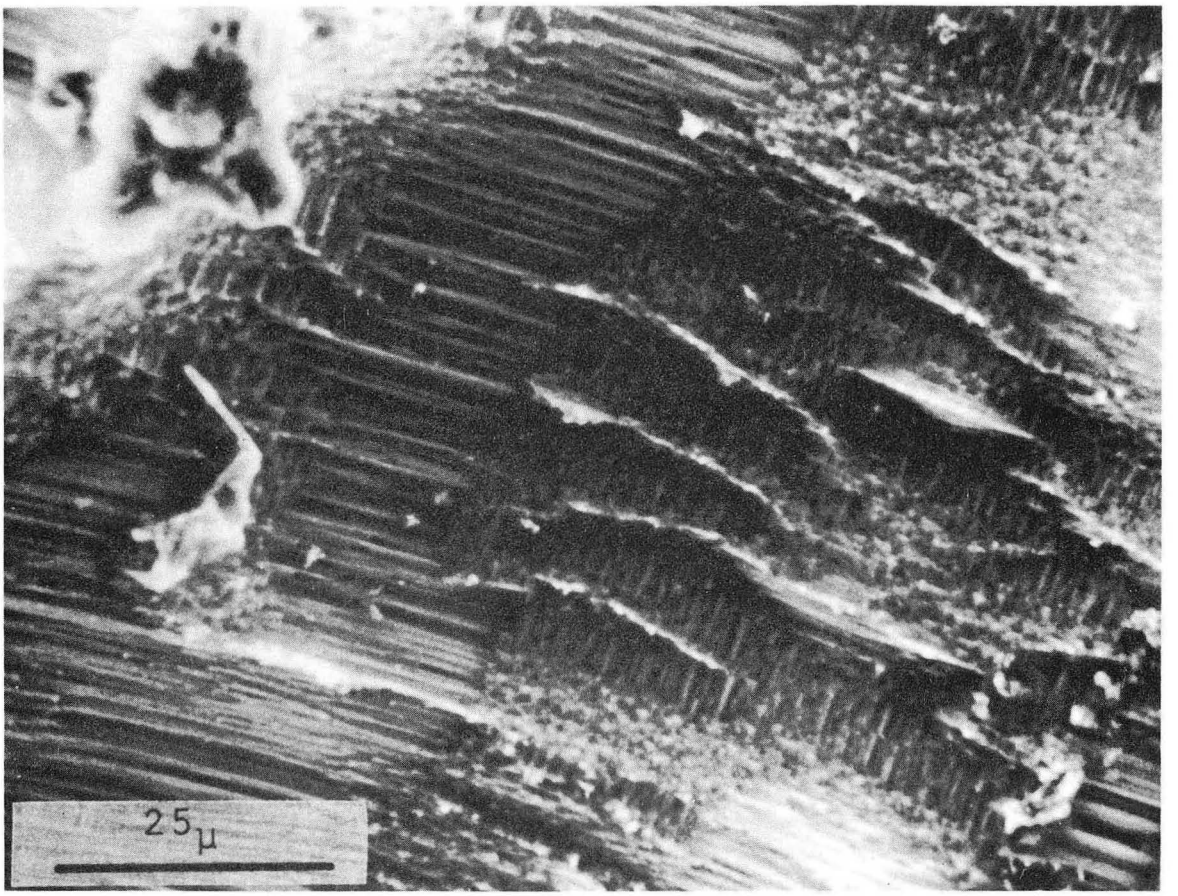

XBB 685-3105

Fig. 7

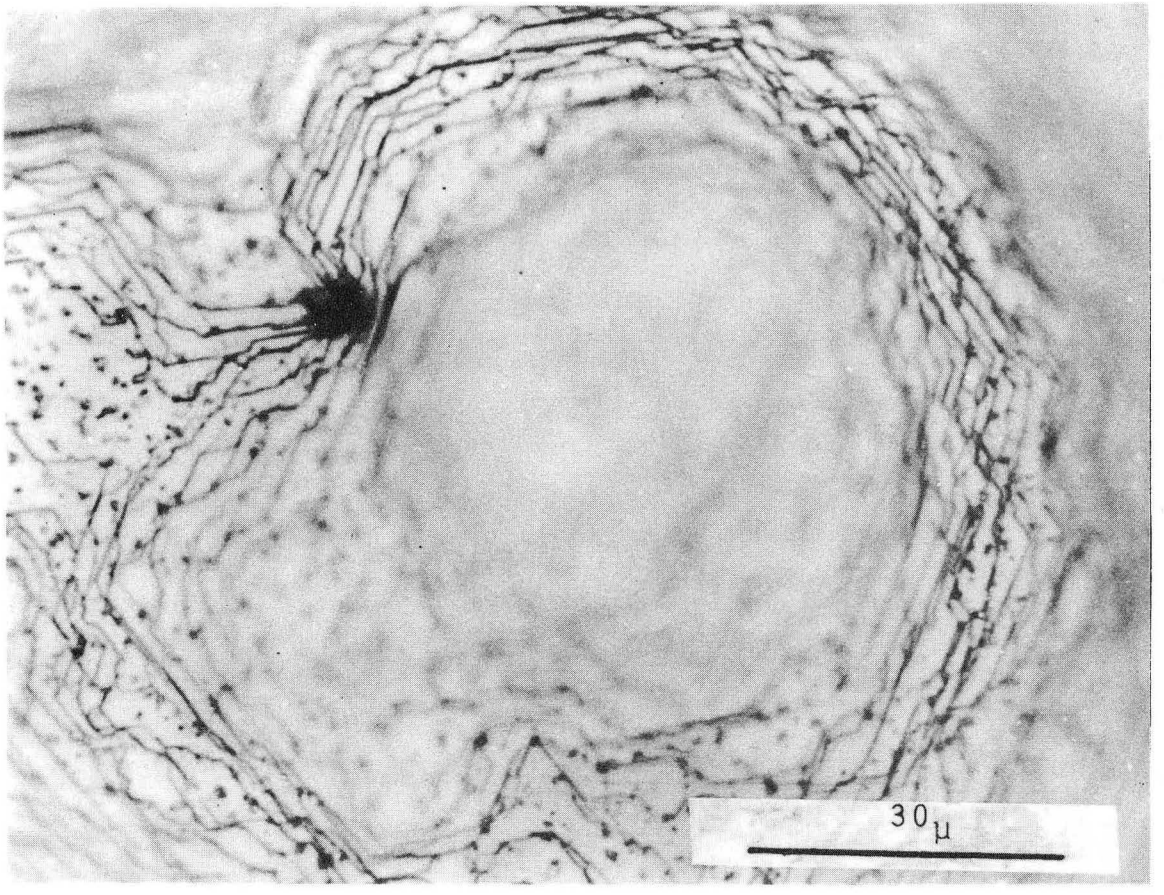

XBB 687-4168

Fig. 8

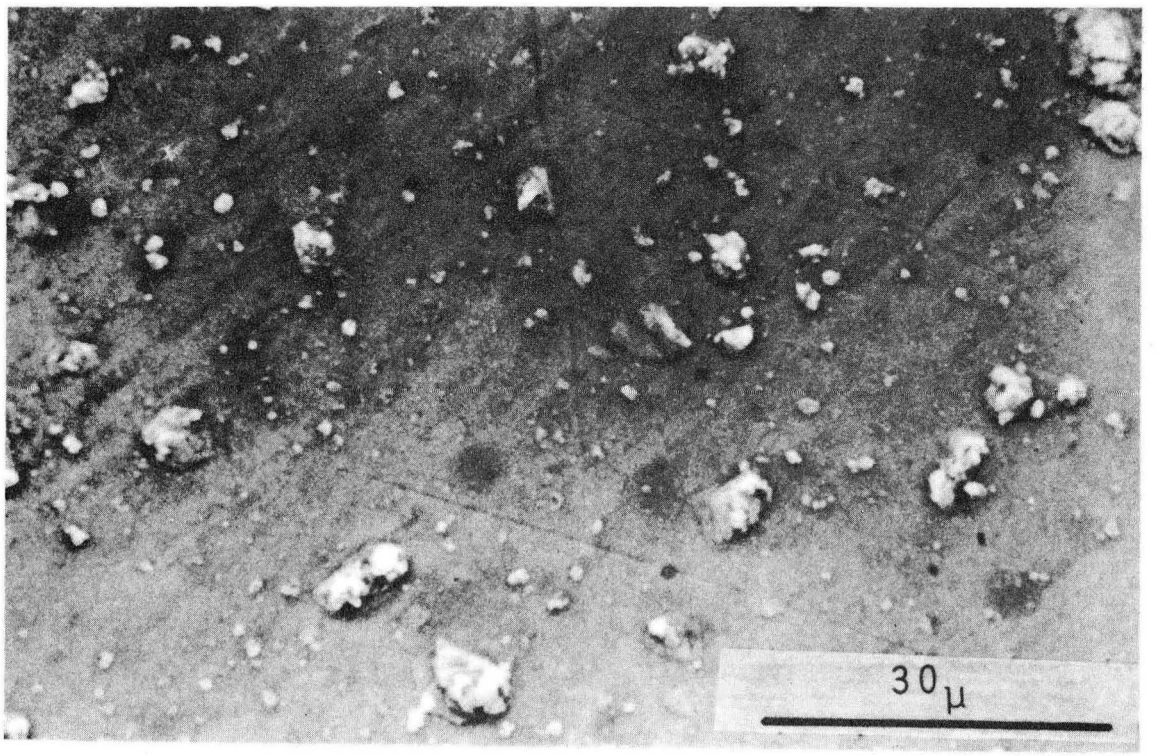

XBB 687-4170

Fig. 9

TECHNICAL INFORMATION DIVISION
LAWRENCE RADIATION LABORATORY
UNIVERSITY OF CALIFORNIA
BERKELEY, CALIFORNIA 94720